Deep–Sea Research I 117 (2016) 51–60

Contents lists available at ScienceDirect

Deep–Sea Research I

journal homepage: www.elsevier.com/locate/dsri

Physical-biological coupling in the Amundsen Sea, Antarctica: Influence of physical factors on phytoplankton community structure and biomass

Youngju Lee, Eun Jin Yang*, Jisoo Park, Jinyoung Jung, Tae Wan Kim, SangHoon Lee

Division of Polar Ocean Environment, Korea Polar Research Institute, 26, Songdomirae-ro, Yeonsu-gu, Incheon 21990, Republic of Korea

ARTICLE INFO

Keywords:
Phytoplankton
Phaeocystis antarctica
Diatoms
Amundsen Sea
Polynya

ABSTRACT

To understand the spatial distribution of phytoplankton communities in various habitats in the Amundsen Sea, western Antarctica, a field survey was conducted at 15 stations during the austral summer, from December 2013 to January 2014. Water samples were analyzed by microscopy. We found high phytoplankton abundance and biomass in the Amundsen Sea polynya (ASP). Their strong positive correlation with water temperature suggests that phytoplankton biomass accumulated in the surface layer of the stratified polynya. In the ASP, the predominant phytoplankton species was *Phaeocystis antarctica*, while diatoms formed a major group in the sea ice zone, especially *Fragilariopsis* spp., *Chaetoceros* spp., and *Proboscia* spp. Although this large diatom abundance sharply decreased just off the marginal sea ice zone, weakly silicified diatoms, due to their high buoyancy, were distributed at almost all stations on the continental shelf. *Dictyocha speculum* appeared to favor the area between the marginal sea ice zone and the ASP in contrast to cryptophytes and picophytoplankton, whose abundance was higher in the area between the continental shelf and the open ocean of Amundsen Sea. Several environmental factors were found to affect the spatial variation of phytoplankton species, but the community structure appeared to be controlled mainly by the seawater density related to sea-ice melting and water circulation in the Amundsen Sea.

1. Introduction

The Southern Ocean is a net sink for atmospheric CO_2 uptake at annual timescales. With its high primary productivity (Arrigo et al., 2008), it accounts for 20% of CO_2 uptake in the global ocean (Takahashi et al., 2009). Phytoplankton blooms occupy local areas of reduced ice cover that generally form due to offshore katabatic winds and seasonal ice melt and appear in the austral summer in coastal polynyas (Tremblay and Smith, 2007). The higher insolation and thinner sea ice during the growth season allow the penetration of sufficient irradiance to drive photosynthesis in this continental shelf area. The seasonal variation of phytoplankton biomass and primary production in Antarctic shelf waters play an important role in the biogeochemical cycles of the Southern Ocean (Hoppema and Anderson, 2007).

Studies of the dynamics of phytoplankton in Antarctic coastal waters have shown that both diatoms and the prymnesiophyte *Phaeocystis antarctica* form massive blooms during different seasons and in different areas (Arrigo et al., 1999; Smith et al., 2010). The dominance of these two major groups and the controlling mechanisms differ from year to year, which complicates predictions regarding their distribution (Smith Jr et al., 2006). Most studies have thus far focused on regions in the Ross Sea, the Weddell Sea, and eastern Antarctica (Arrigo et al., 1999; Lancelot et al., 1993; Wright et al., 2010).

The Amundsen Sea polynya (ASP) is the most productive of the 37 identified coastal polynya systems in the Antarctic when assessed per unit area (Arrigo and van Dijken, 2003). The Amundsen Sea is a current hot spot of rapidly thinning ice shelves in Antarctica, a phenomenon attributed to global warming (Pritchard et al., 2012; Rignot et al., 2008). The basal melting of ice shelves in the ASP is accelerated by the intrusion of modified circumpolar deep water (mCDW) (Rignot et al., 2013), which could lead to changes in water column stratification and water circulation, coastal upwelling, and iron (Fe) supply (Gerringa et al., 2012; Rignot et al., 2013; Wang et al., 2014).

In recent studies, the distribution and physiology of the phytoplankton community have been assessed based on measurements of photosynthetic pigments using CHEMTAX (CHEMical TAXonomy) and phytoplankton biomass and primary production derived from satellite data in the Amundsen Sea (Arrigo et al., 2012; Fragoso and Smith Jr, 2012). The results of those studies have shown that the distribution of phytoplankton in the Amundsen Sea is influenced by

* Corresponding author.
E-mail address: ejyang@kopri.re.kr (E.J. Yang).

http://dx.doi.org/10.1016/j.dsr.2016.10.001
Received 9 January 2016; Received in revised form 4 October 2016; Accepted 5 October 2016
Available online 06 October 2016
0967-0637/ © 2016 Elsevier Ltd. All rights reserved.

water column stratification, Fe supply, and grazing (Alderkamp et al., 2012b; Mills et al., 2012). In most of these studies, high-performance liquid chromatography (HPLC) was used to examine major species, such as *Phaeocystis antarctica* and diatom groups. Phytoplankton responses to environmental changes are found to differ in terms of both the various groups and individual species (Rose et al., 2009; Xu et al., 2014). Thus, both the distribution and response of whole phytoplankton assemblages, including minor groups, in the rapidly melting Amundsen Sea need to be understood before phytoplankton responses to rapid climate change can be accurately predicted. Accurate information on the phytoplankton communities can be acquired by microscopy. Although this approach is time-consuming and requires a high level of expertise, it provides the basic and detailed information needed to understand phytoplankton ecology and physiology.

We herein provide a first step towards an improved understanding of the spatial variation of phytoplankton species in the Amundsen Sea. In this microscopy-based study, the distribution of the phytoplankton communities was investigated in four distinct habitats [the oceanic area (OA), the ASP, the marginal sea ice zone (MSIZ), and the Dotson ice shelf (DIS)] to elucidate its spatial distribution in response to the changing physical and chemical environment occurring in response to the rapidly melting Amundsen Sea.

2. Materials and methods

2.1. Field survey and sample processing

A field survey was conducted onboard the Korean IBRV Araon in the ASP and the surrounding seas during the austral summer from 31 December 2013–14 January 2014 (Fig. 1). Vertical profiles of sea water temperature, salinity, water pressure, water density (sigma-t), and photosynthetic available radiation (PAR) were obtained at 15 stations from casts of a Seabird 911plus model CTD (Sea-Bird Electronics, USA). The mixed layer depth (MLD) was defined as the depth at which the density change exceeded 0.05 kg m^{-3} relative to the reference value at 10 m depth (Venables and Moore, 2010). The euphotic depth was estimated as the depth at which the PAR was 1% of its surface value. Sea ice concentration data were obtained from the Nimbus-7 scanning multichannel microwave radiometer and Defense Meteorological Satellite Program special sensor microwave/imager–special sensor microwave imager/sounder passive microwave data (Cavalieri et al., 1996).

Water samples collected from 4 to 5 layers in the upper 100 m were either analyzed for nutrients and chlorophyll-a (Chl-a) concentrations or used for microscopy. The samples were obtained using a 10 L PVC Niskin water sampler attached to a CTD rosette system. The analyzed nutrients were nitrate+nitrite, ammonium, phosphate, and silicate. Their concentrations were measured onboard using a Bran and Luebbe model Quatro auto-analyzer according to the manufacturer's instructions (Lee et al., 2015). Chl-a was determined onboard at each depth using samples immediately filtered through glass-fiber filter paper (47 mm; Gelman GF/F), extracted with 90% acetone for 24 h (Persons et al., 1984), and then measured in a fluorometer (Trilogy, Turner Designs, USA), previously calibrated against pure Chl-a (Sigma).

To estimate phytoplankton abundance, water samples from the Niskin bottles were subsampled using 200 mL high-density polyethylene bottles, preserved with glutaraldehyde (final concentration 1%), and stored at 4 °C until processed as follows: Sample volumes of 50–150 mL were filtered through Nuclepore filters (0.8 μm pore size, black, 25 mm diameter) until 5 mL were remaining in the filtration tower.

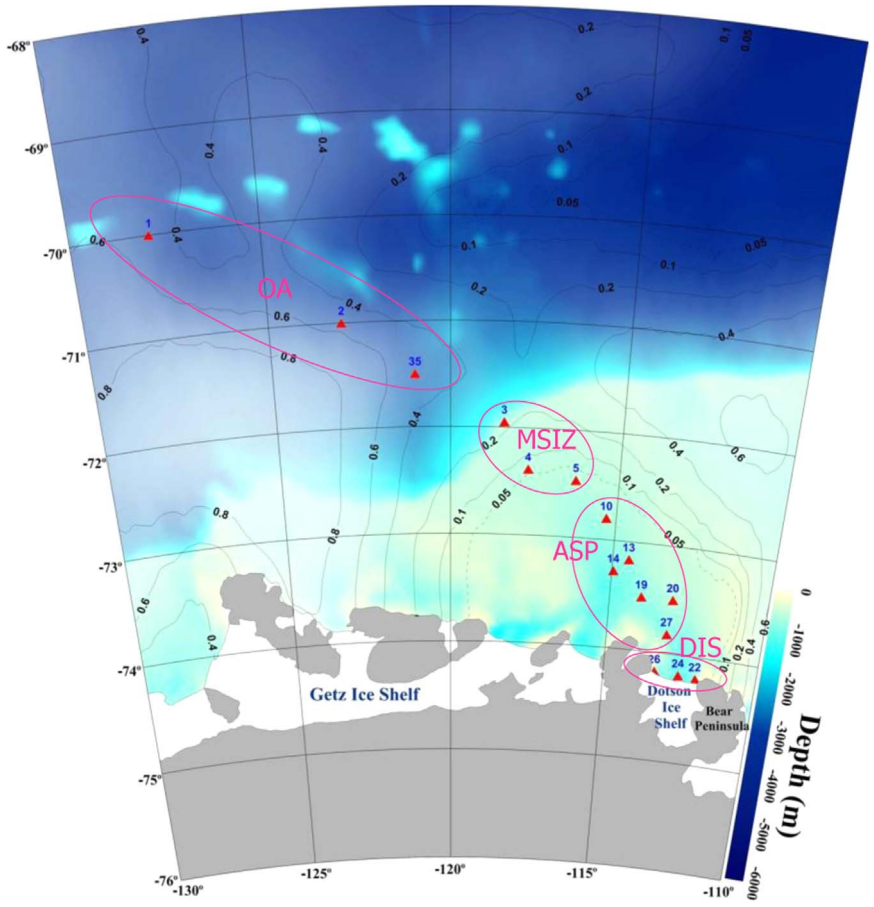

Fig. 1. Sampling stations and the mean sea ice concentration (grey contour line, ×100%) from December 31, 2013 to January 14, 2014 with bathymetry of the study area, which was geographically divided into 4 habitats: oceanic area (OA), marginal sea ice zone (MSIZ), Amundsen Sea polynya (ASP), and Dotson Ice Shelf (DIS) in the Amundsen Sea, Antarctica.

Concentrated DAPI (50 μg mL^{-1} final concentration) was then added to this remaining volume, which was also filtered after a brief (5 s) incubation (Taylor et al., 2011; Yang et al., 2015). The filters were mounted on glass slides with immersion oil and cover slips. Microphytoplankton (> 20 μm), nanophytoplankton (5–20 μm), and picophytoplankton (2–5 μm) and dinoflagellates were enumerated using epifluorescence microscopy with blue light excitation (Olympus, BX 51). Phytoplankton was distinguished from heterotrophs by the presence of chlorophyll, which was visualized as red fluorescence under blue light illumination. Most *Phaeocystis antarctica* was present as solitary flagellated cells ranging in size from 2 to 6 μm. The cells were counted in random fields at magnifications of 200–1600×until a total of 50 fields or 300 cells had been observed. Phytoplankton cell dimensions were measured to the nearest 1 μm during the microscopy observations. The values were used for subsequent estimations of biovolume according to the geometric shapes of the cells. Carbon (C) biomass was estimated from the cell biovolume using modified Eppley equations (Hillebrand et al., 1999) as follows: for diatoms, $\log_{10}$ C(pg) =0.76 $\log_{10}$[cell volume (μm^3)]−0.352; for other phytoplankton, $\log_{10}$ C(pg)=0.94 $\log_{10}$[cell volume (μm^3)]−0.60. The conversion factor was used to transform the cell numbers of solitary *Phaeocystis antarctica* into carbon biomass (3.33 pgC $cell^{-1}$) (Mathot et al., 2000).

2.2. Data analysis

The statistical analyses were carried out using R3.1.3 (R Development Core Team, http://www.r-project.org) unless otherwise stated. The geographic map and figures were created using ODV software (R. Schlitzer, Ocean Data View, http://odv.awi.de, 2011).

The spatial environmental status of the four habitats was summarized using principal components analysis (PCA) based on log-transformed/normalized abiotic data from the surface layer. The differences between groups of samples were assessed by ANOSIM (Clarke and Gorley, 2006). Species abundance data were broken down into univariate measures of community structure to identify trends. These measures were species richness (Margalef *D*), species diversity (Shannon-Wiener *H′*), and evenness (Pielo's *J′*). Phytoplankton species were subdivided according to their similarity to distinguish those species closely related to each other. Phytoplankton groups were classified with a similarity dendrogram (Bray Curtis, complete linkage) using the square-root-transformed dominance rate of 24 ranked phytoplankton species. The spatial differences in phytoplankton communities were visualized with a canonical analysis of principal coordinates (CAP) based on a discriminant analysis (Anderson and Willis, 2003) using the CAPdiscrim function (BiodiversityR package) with Bray-Curtis similarities from log-transformed species-abundance data. The correlation between biotic and abiotic data was tested according to the Mantel statistic using the mantel function (vegan package). To examine the relationship between environmental factors and phytoplankton in the study area, Spearman's rank correlation was used with the normalized abiotic data and the log-transformed biotic data because most of the data did not satisfy assumptions of normality. BIOENV analysis (Clarke and Ainsworth, 1993) was used in a multivariate analysis to explore the relationships between environmental variables and phytoplankton species abundance (Primer, V5.0).

3. Results

The study area was geographically divided into four habitats: OA (stations 1, 2, and 35), MSIZ (stations 3, 4, and 5), ASP (stations 10, 13, 14, 19, 20, and 27), and DIS (stations 22, 24, and 26) (Fig. 1).

3.1. Environmental characteristics of the Amundsen Sea habitats

The environmental variables of the four habitats showed distinct characteristics (Fig. 2 and Table 1). The seawater temperature and salinity distribution near the surface were controlled by the sea ice conditions in the Antarctic area. Because of atmospheric heating by

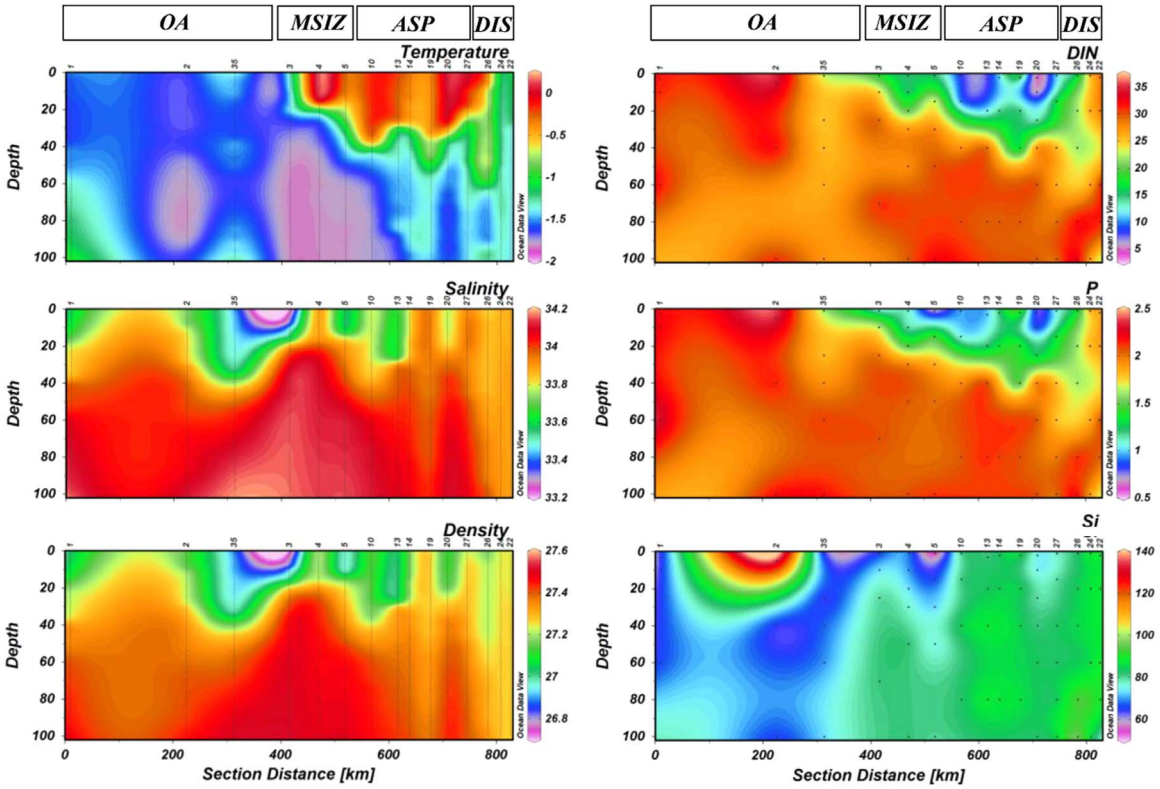

Fig. 2. Vertical distribution of water temperature (°C), salinity, water density (sigma-t), dissolved inorganic nitrogen (DIN), phosphate (P), and silicate (Si) concentrations (μM) along the transect from the oceanic area to ice shelf in the Amundsen Sea. See Table 2 for abbreviations.

Table 1
Environmental variables (mean ± SD) in surface layers of the 4 geographical areas.

	Oceanic area	Marginal sea ice zone	Amundsen Sea polynya	Dotson ice shelf
Temperature (°C)	−1.50 ± 0.13	−0.47 ± 0.76	−0.14 ± 0.17	−0.87 ± 0.43
Salinity	33.58 ± 0.15	33.56 ± 0.33	33.81 ± 0.11	33.85 ± 0.02
MLD (m)	21.33 ± 6.11	15.33 ± 2.31	34.00 ± 11.05	115.67 ± 45.71
Z_{eu} (m)	36.57 ± 8.40	15.17 ± 2.73	11.17 ± 0.94	16.73 ± 3.78
PO_4 (μM)	2.06 ± 0.38	0.98 ± 0.23	1.06 ± 0.21	1.67 ± 0.30
NO_2+NO_3 (μM)	29.55 ± 5.89	15.60 ± 1.79	9.66 ± 3.83	23.12 ± 6.16
NH_4 (μM)	ND	0.54 ± 0.19	0.17 ± 0.14	0.06 ± 0.05
SiO_2 (μM)	87.85 ± 40.91	62.95 ± 7.86	80.26 ± 3.96	86.21 ± 2.80
Surface Chl-a (μg L^{-1})	0.67 ± 0.69	4.90 ± 0.90	8.89 ± 1.11	4.06 ± 0.97

MLD, mixed layer depth; Z_{eu}, euphotic depth.

solar radiation, sea surface temperatures in the ASP (mean, −0.14 °C) and DIS (−0.87 °C) were higher than in the OA (−1.50 °C), where a heavy sea ice cover was observed. The MSIZ, the transition area between the OA and the ASP, includes the sea ice zone and the marginal sea ice zone near the shelf break. Surface warming by incoming solar radiation in the MSIZ produced lower sea ice concentration than in the OA. This warm water accelerated the melting of the sea ice in this area. Therefore, the minimum salinity in the surface layer was found at the MSIZ and reflected the inflow of meltwater from sea ice.

The concentration of macronutrients, including dissolved inorganic nitrogen (DIN) and phosphate, were relatively low in the upper ocean of the ASP, where Chl-a concentrations were high (average of 8.89 μgL^{-1}). Vertically, the Chl-a concentration was significantly higher in the surface layer of the continental shelf but decreased sharply with increasing depth (Fig. 6). The amount of light, after its penetration of the surface layer, was such that 99.9% of the incident light was attenuated within a depth of 20–30 m in the water column of the Amundsen continental shelf area (data not shown). The euphotic depth in the DIS was deeper (average of 16.73 m) than in the ASP (11.17 m), indicating better underwater light conditions in the shelf area (Fig. 3). The MLD was higher in the DIS (average of 115.67 m) than in the ASP (34.00 m), MSIZ (15.33 m), or OA (21.33 m). In the OA, the euphotic depth was deeper than the MLD (Fig. 3).

The results of the PCA using the surface data set are shown in Fig. 4. The first PCA axis explained a large proportion (45.5%) of the total environmental variability, separating the ASP from the OA. The second axis explained 36.1% of the total environmental variability, discriminating three areas in the continental shelf: the ASP, the MSIZ, and the DIS. The temperature vector indicated the stations in the ASP, and the vectors of phosphate, nitrogen, and euphotic depth the stations in the OA. The ammonium vector was indicative of the stations in the MSIZ, and the vectors of density, salinity, MLD, and silicate of the stations in the DIS. The discrimination of geographic areas in the PCA biplot (ANOSIM, r =0.671, $p < 0.001$) allowed the recognition of distinct differences in the spatial distribution of environmental parameters in the study area.

3.2. Phytoplankton community structure

Phytoplankton abundance in the study area was generally dominated by *Phaeocystis antarctica*, which had an average dominance percentage of 76% (Figs. 5 and 6). The dominance percentage of *Phaeocystis antarctica* with respect to phytoplankton abundance were less at stations 1 and 2 of the OA (< 22%) than in the ASP and the DIS (> 93%). In the MSIZ, diatoms and *Phaeocystis antarctica* co-dominated, with relative abundances of 17–65% and 33–81%, respectively. Diatoms accounted for 67–91% of the phytoplankton carbon biomass, however, because of their larger size and higher carbon content compared to *Phaeocystis antarctica*.

Despite the dominance of *Phaeocystis antarctica* and diatoms in the study area, minor groups showed distinct spatial distributions (Fig. 6). The abundance of the chrysophyte *Dictyocha speculum* was higher in the MSIZ and the ASP than in the OA and DIS, with the highest abundance recorded in the surface layer at Station 4. Dinoflagellates, including *Gymnodinium* spp. and *Prorocentrum* spp., were more abundant in the continental shelf area than in the OA. Within the former, however, the abundance of dinoflagellates was relatively low in the DIS. *Pyramimonas* spp., a genus within the prasinophytes, had a relatively high abundance in the OA but was also found in the ASP. Nanophytoflagellates (< 20 μm) and cryptophytes were also of high abundance in the OA, with the highest abundance of the latter detected at Station 1.

A species similarity analysis distinguished four groups of phytoplankton (Fig. 7): (a) pico- and nanophytoplankton, such as *Phaeocystis antarctica*, *Fragilariopsis cylindrus/ nana*, and picoflagellates (< 2 μm); (b) nanophytoflagellates, such as *Pyramimonas* sp., cryptophytes, and unidentified nanoflagellates, which were of relatively high abundance in the OA; (c) dinoflagellates and some diatoms; and (d) *Dictyocha speculum* and diatoms mainly distributed in the MSIZ, including *Chaetoceros* spp., *Fragilariopsis cylindrus*, *Plagiotropus gaussi*, *Pseudonitzschia prolongatoides*, and *Cylindrotheca closterium*.

The spatial distribution of univariate variables among the four areas differed (Fig. 8). Evenness and diversity were higher in the OA and MSIZ than in the ASP and DIS, where *Phaeocystis antarctica* predominated in phytoplankton abundance. Species evenness and diversity were highest in the MSIZ, whereas species richness was higher in the upper ocean compared to deeper waters.

A CAP analysis demonstrated clear spatial differences in phytoplankton species-abundance in the Amundsen Sea (Fig. 9). The first canonical axis, which had a large eigenvalue (δ^2 =0.669), distinctly separated phytoplankton communities in the ASP (on the left of the plot) from those in the other three areas, while the second canonical axis (δ^2 =0.281) separated the phytoplankton communities in the the MSIZ (in the right upper quadrant of the plot) in the continental shelf areas.

3.3. Relationship between phytoplankton abundance and environmental factors

A statistical analysis of the entire data set from the 79 samples showed that phytoplankton groups correlated significantly with environmental factors ($p < 0.001$). Specifically, most groups correlated negatively with nutrients, water pressure, and salinity and positively with water temperature and PAR. An exception was *Phaeocystis antarctica*, which was not related to PAR. Phytoplankton biomass (Chl-a) correlated strongly with water temperature (r =0.78, $p < 0.001$).

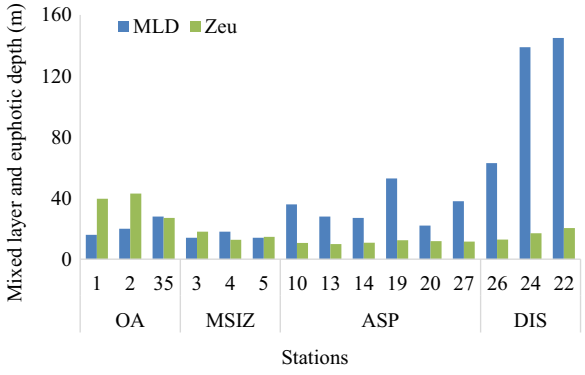

Fig. 3. Cross-shelf distributions of mixed layer depth (MLD) and euphotic depth (Zeu) from the oceanic area to ice shelf in the Amundsen Sea.

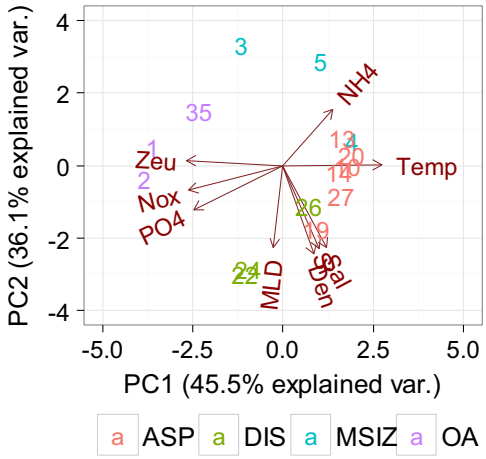

Fig. 4. Principal component analysis (PCA) plots based on log-transformed environmental variable data in the surface layer of four areas. Abbreviations: Temp, temperature; Sal, salinity; NOx, nitrite and nitrate; NH_4, ammonium; PO_4, phosphate; Si, silicate; Den, water density; MLD, mixed layer depth; Zeu, euphotic depth.

A Mantel test also showed consistency in the spatial variability between the biotic and abiotic data from the PCA and CAP analyses of the study area (p=0.001).

A BIOENV analysis was carried out to evaluate the potential environmental factors that influenced the phytoplankton community structure (Table 3). Water density, nutrients, water temperature, and salinity were the subsets that best correlated with the similarity of phytoplankton species abundance in the study area ($p < 0.01$).

4. Discussion

4.1. Spatial distributions of the phytoplankton community in the Amundsen Sea

It is well established that *Phaeocystis antarctica* and diatoms differ in their spatial and temporal distributions in Antarctic coastal waters (Arrigo et al., 1998; Goffart et al., 2000). Several studies on the autecology of some key species in these groups documented the importance of environmental factors, such as light, MLD, seeding from sea ice, Fe, sinking, and grazing, all of which were suggested to control the phytoplankton distribution in the Ross Sea (Alderkamp et al., 2012a; Arrigo et al., 2010; Kropuenske et al., 2009; Xu et al., 2014). The few studies on the Amundsen Sea suggested that light, Fe, and seeding from sea ice were important environmental factors influencing the phytoplankton community. However, those studies were based on photosynthetic pigments analysis (Alderkamp et al., 2012b; Arrigo et al., 2014; Fragoso and Smith Jr, 2012), whereas in our work, the spatial distribution of the phytoplankton community in various habitats was evaluated microscopically, which allowed us to discern species differences among the assemblages, particularly of diatoms. Microscopy also yielded information on the size composition of the

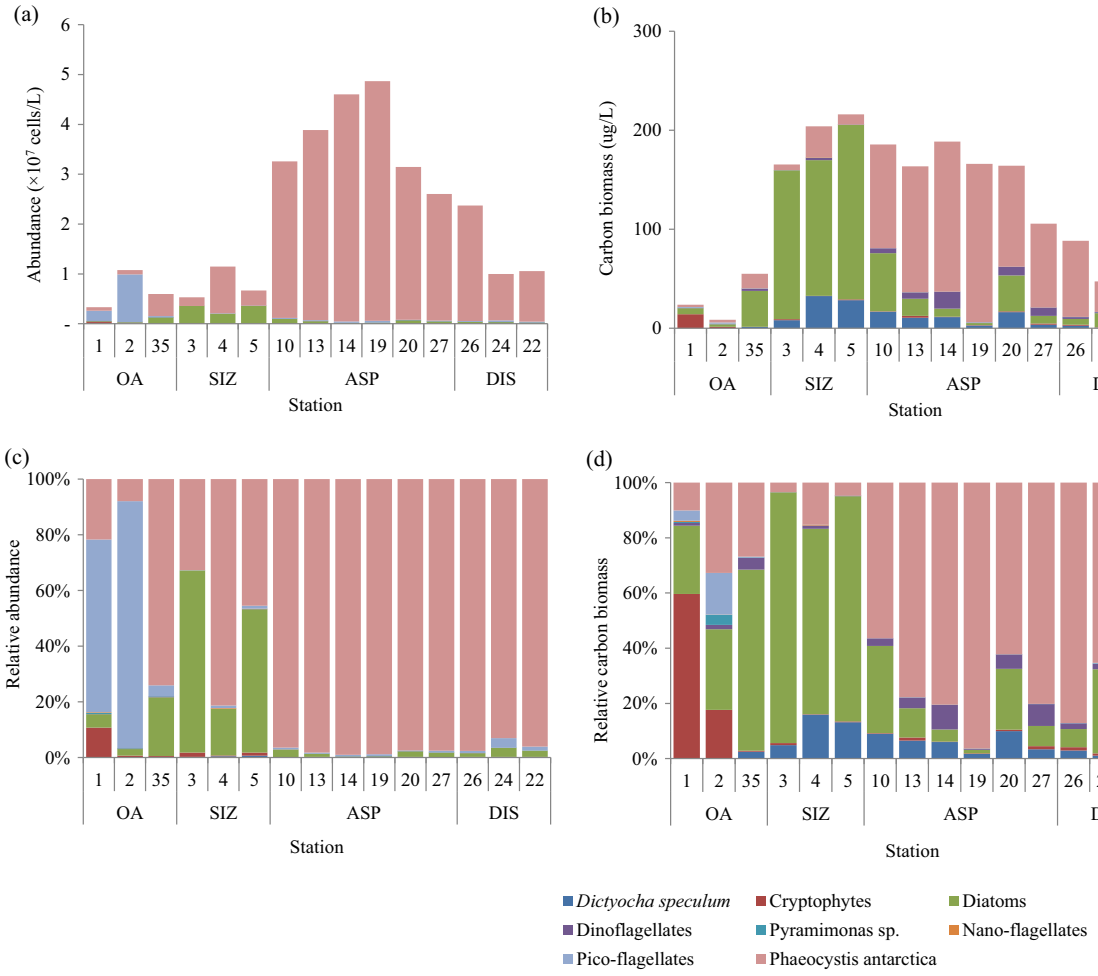

Fig. 5. Cross-shelf contribution of (a and c) surface abundance ($cells L^{-1}$) and (b and d) carbon biomass ($\mu g CL^{-1}$) of the phytoplankton groups from the oceanic area to ice shelf in the Amundsen Sea.

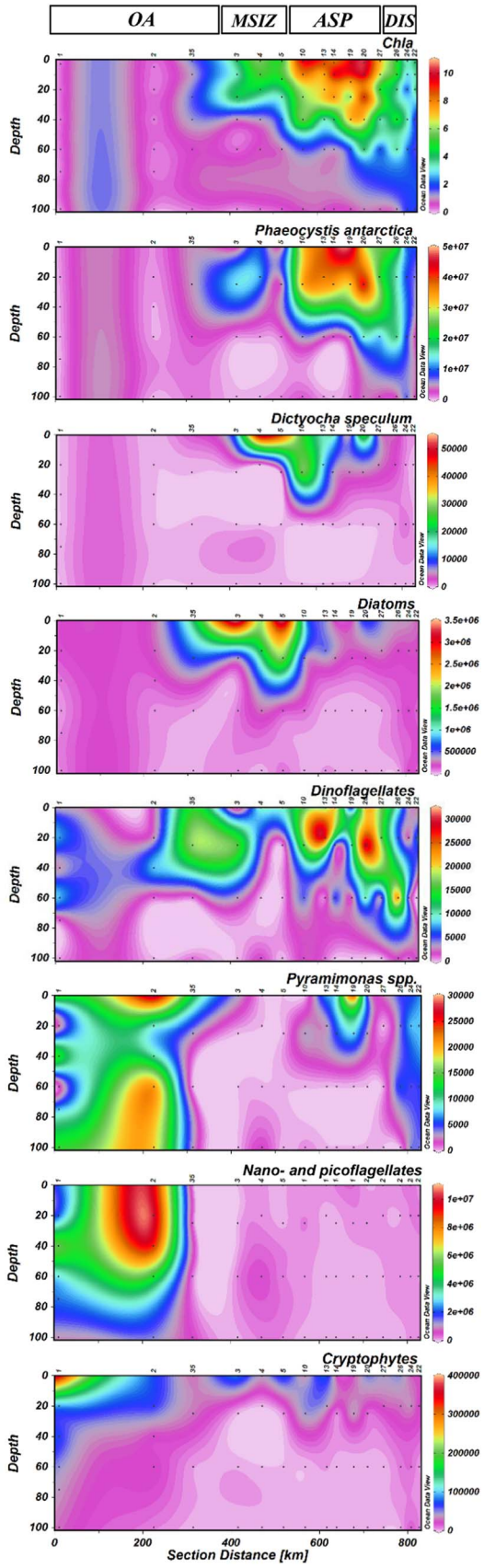

Fig. 6. Vertical distribution of chl-a (μgL^{-1}) and phytoplankton group abundance ($cellsL^{-1}$) along the transect from the oceanic area to ice shelf in the Amundsen Sea.

phytoplankton species. Our results confirmed the predominance of *Phaeocystis antarctica* and diatoms in the ASP and MSIZ, respectively, in the Amundsen Sea. However, the species abundance data also provide us with detailed information on phytoplankton ecology and physiology. For example, the large diatoms *Proboscia* spp., *Tropidoneis* spp., and *Corethron pennatum* were minor species in terms of abundance, but they accounted for 35% of the phytoplankton carbon biomass in the surface layer of the MSIZ, and their abundance decreased sharply just outside the MSIZ, at station 10. By contrast, colonies of the pelagic diatoms *Chaetoceros* spp. and *Thalassiosira* spp. were mainly distributed in the MSIZ, but their distribution expanded slightly to the ASP. The small diatom *Fragilariopsis cylindrus/ nana* and the weakly silicified diatom *Pseudonitzschia prolongatoides* were detected at all stations in the Amundsen Sea, although both were minor species in the study area except in the MSIZ. Smaller cells with higher surface area-to-volume ratios advantage benefit from reduced sinking rates after seeding from sea ice in spring. Taken together, these results show that diatoms were mainly distributed in the MSIZ but, according to their greater buoyancy, their distribution expanded to include the whole continental shelf area. This was demonstrated before by microscopic analyses of phytoplankton in the Weddell Sea and Ross Sea (Garrison et al., 2003; Kang et al., 2001).

Diatoms and *Phaeocystis antarctica* play different roles in the biogeochemical cycle of Antarctic coastal waters. Compared to diatoms, *Phaeocystis antarctica* is better able to draw down atmospheric CO_2 (Arrigo et al., 1999). Diatoms, however, with their faster sinking rate compared to *Phaeocystis antarctica*, sink rapidly to depth (Asper et al., 1992). A sediment trap study in the Amundsen Sea showed that particulate organic carbon (POC) flux to depth in the MSIZ was similar to that in the ASP, although the maximum POC was significantly higher in the latter, consistent with the high export efficiency of the diatom-dominant phytoplankton community (Ducklow et al., 2015; Kim et al., 2015). These results imply that diatoms play an important role in moving CO_2 from the ocean surface to deeper layers in the Antarctic waters. Variations in the size and buoyancy of the diatom assemblage result in differences in their sinking rates which can affect the downward carbon flux (Eppley et al., 1967). In previous studies in the Amundsen Sea, diatoms were investigated as one CHEMTAX group (Chl-a) based on their photosynthetic pigments, despite the fact that diatoms comprise of several species that differ in their spatial distribution according to the size and buoyancy of their cells. This oversimplification can be avoided by microscopic analyses, which provides the information needed to understand the relationship between biogeochemical cycles and phytoplankton communities, especially diatom assemblages in the Antarctic continental shelf.

Moreover, microscopy also allows investigations of minor species. For example, the ecology and physiology of the chrysophyte *D. speculum* in Antarctic coastal waters are practically unknown. A previous report suggested that this species favors the shallow MLD of the Ross Sea (Fragoso and Smith Jr, 2012). In this study, *D. speculum* was mainly distributed in the surface layer of the area between the MSIZ and the ASP, where the MLD is shallow. The abundance of *D. speculum* correlated strongly with both water density and the PAR ($p < 0.001$), suggesting that MLD, water density, and light are important environmental variables determining the spatial distribution of *D. speculum* in Antarctic coastal waters. Small flagellates, including *Pyramimonas* spp., cryptophytes, and nano- and pico-flagellates, were detected in the surface layer of almost all stations, but their abundance and dominance with respect to phytoplankton abundance were higher in the OA than in the continental shelf area. Thus, the OA was distinguished by the dominance of small flagellates from the Amundsen continental shelf area. Cryptophytes had the highest dominance in the phytoplankton biomass at Station 1. Cryptophyte blooms have been reported in the Ross Sea (Arrigo et al., 1999) and Antarctic Peninsula (Mendes et al., 2013). The distribution of these

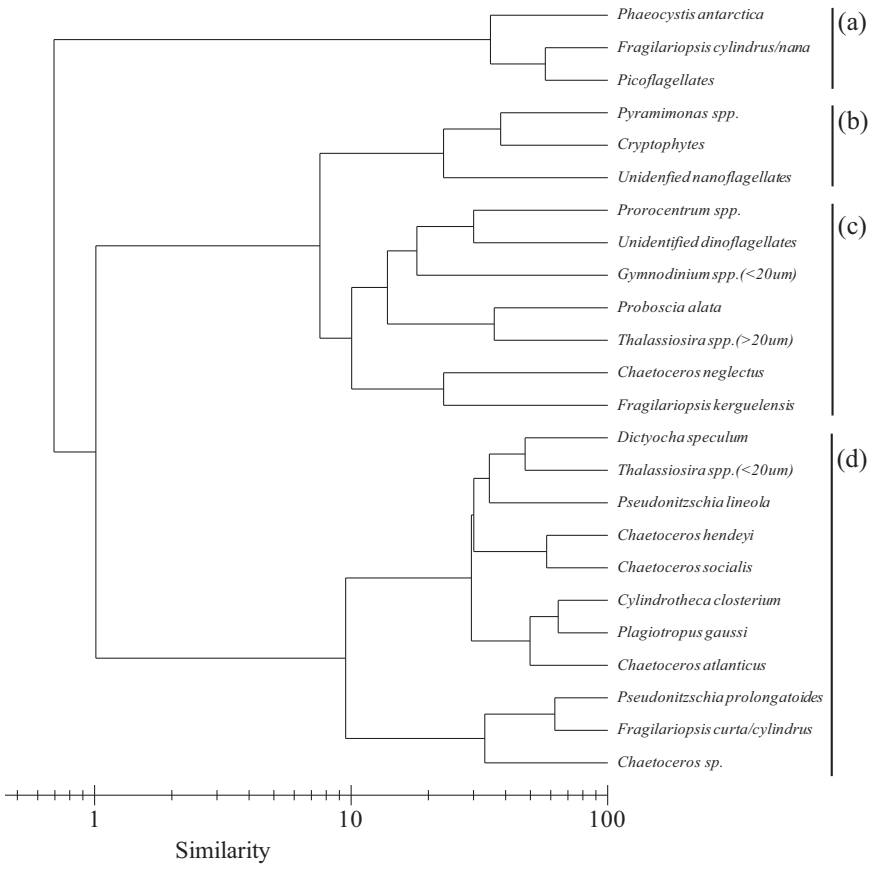

Fig. 7. Phytoplankton group classification in a similarity dendrogram (Bray Curtis, complete linkage) using square root transformed dominant rate of 24 rank phytoplankton species. Phytoplankton is divided into four groups: (a) pico- and nanophytoplankton, (b) nanophytoflagellates, (c) dinoflagellates and diatoms, and (d) diatoms and *Dictyocha speculum*.

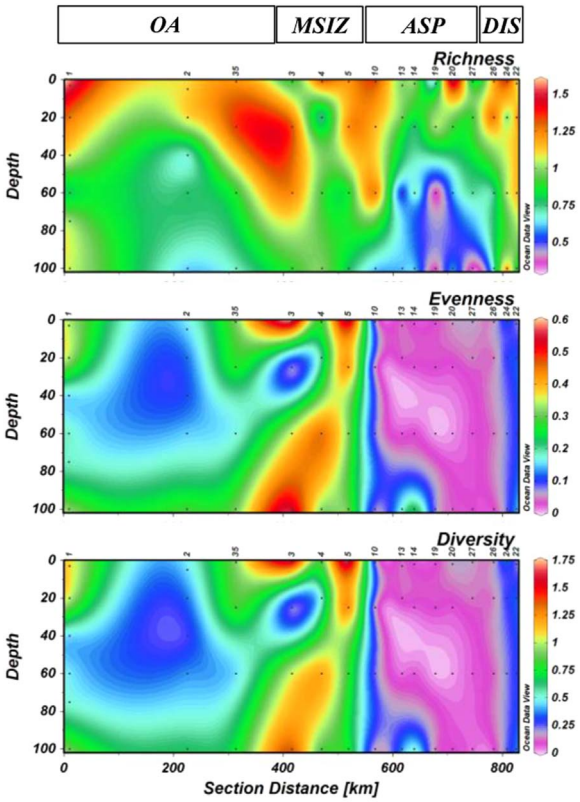

Fig. 8. Vertical distribution of richness, evenness, and diversity index along the transect from the oceanic area to the ice shelf in the Amundsen Sea.

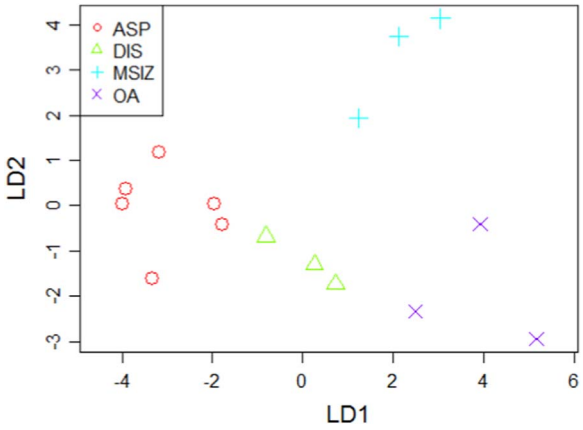

Fig. 9. Canonical analysis of principal coordinates (CAP) analysis plot of linear discriminants (LDs) 1 and 2 on Bray-Curtis similarities from depth-integrated and log-transformed species-abundance data in the Amundsen Sea.

species may therefore be associated with the low salinity of the glacial melting area and MLD, along with stratification and the ambient light field in the area between the coastal and offshore stations (Garibotti et al., 2005). In this study, the water mass in the OA, where cryptophytes and pico- and nanoflagellates dominated in terms of phytoplankton biomass and abundance, was characterized by lower temperature, lower salinity, and a better underwater light field than that in the ASP. These features were opposite to the environmental features of the MSIZ and the intermediate area. An increasing dominance of cryptophytes that occurred in tandem with glacial melt runoff and reduced sea surface salinities was reported in the Antarctic Peninsula (Moline et al., 2004). Therefore, the abundances and

Table 2
Spearman's rank correlations between environmental variables and phytoplankton group abundance in the Amundsen Sea (*p < 0.05, **p < 0.01, ***p < 0.001).

	Temp	Salinity	Density	Pressure	PAR	DIN	P	Si	Chl-a
Phaeocystis antarctica	0.74***	−0.53***	−0.58***	−0.47***	0.19	−0.82***	−0.83***	0.23	0.94***
Diatoms	0.53***	−0.71***	−0.73***	−0.78***	0.65***	−0.54***	−0.63***	−0.30*	0.59***
Dictyocha speculum	0.80***	−0.62***	−0.67***	−0.59***	0.46***	−0.79***	−0.81***	−0.02	0.76***
Cryptophytes	0.45***	−0.72***	−0.72***	−0.70***	0.77***	−0.2	−0.22	−0.35**	0.2
Dinoflagellates	0.54***	−0.56***	−0.61***	−0.59***	0.45***	−0.54***	−0.55***	−0.19	0.61***
Pyramimonas spp.	0.16	−0.41***	−0.39**	−0.35**	0.55***	0.07	0.07	−0.05	−0.06
Nanoflagellates (2–20 μm)	−0.33**	0.16	0.18	0.01	0.08	0.40**	0.37**	−0.40**	−0.39**
Picoflagellates (< 2 μm)	−0.17	−0.07	−0.05	−0.27*	0.41***	0.28**	0.33**	−0.41***	−0.39**

Temp, temperature; PAR, photosynthetically active radiation; DIN, dissolved inorganic nitrogen; P, phosphate; Si, silicate; Chl-a, chlorophyll-a.
* $p < 0.05$.
** $p < 0.01$.
*** $p < 0.001$.

Table 3
Results from a biota-environment (BIOENV) analysis showing the best matches of combinations of environmental variables with variations in phytoplankton abundance.

Number of variations	Best combination of variables	ρ	P
4	Density, DIN, P, Si	0.393	0.01
1	P	0.391	0.01
5	Temperature, Density, DIN, P, Si	0.391	0.01
3	Density, P, Si	0.388	0.01
2	Density, P	0.384	0.01
5	Temperature, Salinity, DIN, P, Si	0.384	0.01
3	Density, DIN, P	0.381	0.01
4	Temperature, Density, P, Si	0.381	0.01
4	Salinity, DIN, P, Si	0.378	0.01
5	Salinity, Density, DIN, P, Si	0.374	0.01

DIN, dissolved inorganic nitrogen; P, phosphate; Si, silicate.

distribution of phytoplankton in the Amundsen Sea, which shows rapid melting of ice shelves because of global warming, should be monitored.

The spatial differences in phytoplankton species composition were also confirmed statistically. A CAP analysis showed clear geographic differences in the Amundsen Sea (Fig. 9), and a PCA revealed differences in the environmental variables in four of its distinct geographic areas (Fig. 4). Together, these results indicate that the spatial distribution of phytoplankton species is influenced by the environmental variables of the different habitats (Mantel test, p=0.001). They also demonstrate that analyses of the whole phytoplankton community provide detailed and sensitive information on the response of phytoplankton to environmental change.

4.2. Physical control on phytoplankton communities in the Amundsen Sea

The best subsets of environmental variables, which explain the spatial distribution of phytoplankton communities, were seawater density, temperature, salinity, and macronutrients (BIOENV) (Table 3). Phytoplankton growth in the Southern Ocean, characterized by high-nutrient low-chlorophyll, is limited by a low Fe concentration and phytoplankton is thus unable to respond to the high macronutrient concentrations (Boyd et al., 2007; de Baar et al., 1990). Average DIN and phosphate concentrations were the lowest (10 μM and 1 μM, respectively) in the surface layer of the ASP where average phytoplankton abundance was the highest, but they still remained high because neither P nor N will be limiting for phytoplankton growth if the DIN and DIP concentrations exceeded 1.0 μM and 0.2 μM, respectively (Dortch and Whitledge, 1992). Therefore, whether nutrients were limiting the phytoplankton distribution during the study period remained unclear. Phytoplankton productivity in the Antarctic polynya is often assumed to be seasonally Fe-limited Unfortunately, iron concentrations were not investigated in this study, but previous bioassay experiments performed in the Amundsen Sea during summer showed that phytoplankton biomass did not respond to Fe additions (Mills et al., 2012). In another experiment in the ASP, the addition of Fe increased phytoplankton growth rates in 4 of the 12 incubations, indicating that Fe availability limits phytoplankton growth rates regionally in the ASP (Alderkamp et al., 2015).

The spatial distribution of phytoplankton biomass (Chl-a) correlated strongly with water temperature in the Amundsen Sea. The highest Chl-a concentration was in the surface layer of the ASP, where *Phaeocystis antarctica* predominated in terms of phytoplankton abundance (r=0.78, $p < 0.001$). Previous studies demonstrated that net community production ($\Delta O_2/Ar$) correlated with water temperature in the Amundsen Sea and suggested that water temperature influenced phytoplankton metabolism (Hahm et al., 2014; Tortell et al., 2012). In the Southern Ocean, the growth of *Phaeocystis antarctica* was not limited at temperatures below 10 °C (Buma et al., 1991), and the growth rates of diatoms and *Phaeocystis antarctica* increased as the water temperature increased to within a range of 2–4 °C (Rose et al., 2009; Schoemann et al., 2005). During the study period, the surface water temperature ranged from −1.62 to 0.23 °C, with a very small spatial variation of within 2 °C in the study area. Nevertheless, there was a strong positive correlation between *Phaeocystis antarctica* and water temperature (Table 2). Phytoplankton growth rate is generally responsive to environmental factors, including temperature, nutrients, iron, and light. Because temperature affects some cellular processes (enzyme-catalyzed reactions) but not others (light harvesting and electron transfer), this results in cellular energy imbalances (Raven and Geider, 1988). This selective effect of temperature on cellular biochemical pathways has implications for mutual limitations, synergistic interactions, and antagonisms with other environmental factors, such as light and Fe supply (Raven and Geider, 1988; Rose et al., 2009). Therefore, despite a small range of variation, we need to prove the independent effect of temperature on the growth rate and physiology of phytoplankton.

Tortell et al. (2012) considered several aspects of warmer water temperature at the polynya surface. In the Amundsen Sea, the relatively warmer mCDW intrudes into the Dotson Trough along the bottom of the shelf, whereas due to basal melting a portion of the water shows upwelling at the end of the trough (Ha et al., 2014; Alderkamp et al., 2015). Upwelling waters from below the DIS will be transported to the ASP surface layer and encounter more sluggish circulation throughout the bay, resulting in increased surface residence times in the ASP. Therefore, the higher surface temperature of the polynya could reflect the time-integrated effect of surface heat fluxes as a result of water circulation (Tortell et al., 2012). A similar mechanism may explain the accumulation of phytoplankton biomass at the ASP surface. Support for this hypothesis comes from this study. The total phytoplankton biomass was significantly higher in the ASP than in the DIS, whereas the phytoplankton group composition in these two areas was similar and dominated by *Phaeocystis antarctica* (Fig. 5). The spatial-dominant patterns of the small diatom *Fragillariopsis cylindrus/nana*

and of picoflagellates were similar to the pattern of *Phaeocystis antarctica*, indicating the continuity of phytoplankton community structure between the DIS and the ASP (Fig. 7). All three of these phytoplankton groups are characterized by small (< 5 μm) cells, which are more buoyant due to their high ratio of surface area-to-volume. While this would presumably explain the accumulation of buoyant phytoplankton in the surface layer of the ASP, there was little difference in the distribution of minor groups between the DIS and the ASP. *D. speculum* was distributed with a high abundance ($> 10^4$ cells L^{-1}) in the surface layer of the ASP but with a relatively low abundance in the DIS ($< 10^3$ cells L^{-1}). The latter suggests light limitation due to the deep MLD, as noted above.

Water density, salinity, and temperature were included by the BIOENV analysis in most of the subsets of environmental variables. Because of the cold temperature of Antarctic waters, the density of seawater is influenced foremost by salinity and secondarily by temperature. In this study, the water density was low in the MSIZ, where freshening was enhanced by sea ice melting. Although *Phaeocystis antarctica* was a predominant species in the continental shelf of the Amundsen Sea, diatoms and *D. speculum* dominated the phytoplankton abundance and biomass of the MSIZ. As discussed above, the slight difference in the distribution of diatoms correlated with their cell sizes in the MSIZ and ASP, suggests the ability of small and/or buoyant species to expand their distribution to the surface layer of the ASP. Microscopic studies conducted in the Weddell Sea and in the Ross Sea had also suggested that the spatial distribution of diatom species is influenced by their buoyancy or by the stability of the water column (Garrison et al., 2003; Kang et al., 2001). Meanwhile, the difference in the photosynthetic response of *P. antarctica* and diatom *F. cylindrus* induced by shallow and deep MLD conditions in the Ross Sea have also been well documented (Mills et al., 2010). However, in this study, environmental variables, such as light at each depth, MLD and euphotic depth did not show strong correlation with phytoplankton species abundance. Nonetheless, carbon biomass of *P. antarctica* dominated in stations where MLD was deeper than the euphotic depth, while diatoms dominated in terms of carbon biomass at stations where both depths were almost same (Table 1). Our results are consistent with previous research based on phytoplankton group biomass using photosynthetic pigments in the Ross Sea (Arrigo et al., 2003). Taken together, the difference in photoacclimation strategies of different phytoplankton groups might be one of the most important factors influencing phytoplankton distribution in the Amundsen Sea. However, the present results rather point to the influence of physical environmental factors, such as water density, sea ice melt, salinity and water temperature as determinants of the spatial variation in the phytoplankton species abundance, particularly of diatoms.

5. Conclusions

In this study, microscopic observations of the spatial distribution of the phytoplankton community provided new insights into the biogeographic differences in the Amundsen Sea. *Phaeocystis antarctica* and diatoms were dominant in the ASP and MSIZ, respectively, but their abundances differed according to their spatial distribution patterns. The distribution of large diatoms was confined to the MSIZ, while more buoyant groups, which included a colony comprising pelagic diatoms, small diatoms, and weakly silicified diatoms, had an expanded distribution area or were found throughout the study area. The area of distribution of the chrysophyte *D. speculum* was between the MSIZ and ASP, whereas cryptophyte abundance was highest in the OA. As observed in this study, the phytoplantkon community structure seemed to be influenced mainly by physical features, such as seawater density, rather than other chemical factors. This is an important consideration in efforts to understand the response of phytoplankton communities to environmental change. The ASP is a rather vulnerable area, where increased basal melting and upwelling have already occurred in response to increased flow of mCDW Ha et al. (2014); Rignot et al. (2013). In addition, water mass circulation, residence time, current speed, and sea ice melt in the Amundsen Sea likely influence not only the community structure but also the biomass of phytoplankton. Further study on the relationships between phytoplankton species composition and environmental variables in the Amundsen Sea will yield the information needed to predict the response of phytoplankton to climate change.

Acknowledgments

The authors thank the captain and crew of the *IBRV* ARAON who were most helpful in all shipboard operations. This research was supported by the Korea Polar Research Institute project (KOPRI; PP 16020) from the Korea Polar Research Institute. Partial support was provided by grants from the K-AOOS Program (KOPRI; PM16040) funded by the Ministry of Oceans and Fisheries, Korea. We greatfully acknowledge the constructive and insightful comments by two reviewers.

References

Alderkamp, A.-C., Kulk, G., Buma, A.G., Visser, R.J., Van Dijken, G.L., Mills, M.M., Arrigo, K.R., 2012a. The effect of iron limitation of the photophysiology of *Phaeocystis antarctica* (Prymnesiophyceae) and *Fragilariopsis cylindrus* (Bacillariophyceae) under dynamic irradiance. J. Phycol. 48, 45–59.

Alderkamp, A.-C., Mills, M.M., van Dijken, G.L., Laan, P., Thuróczy, C.E., Gerringa, L.J.A., de Baar, H.J.W., Payne, C.D., Visser, R.J.W., Buma, A.G.J., Arrigo, K.R., 2012b. Iron from melting glaciers fuels phytoplankton blooms in the Amundsen Sea (Southern Ocean): phytoplankton characteristics and productivity. Deep-Sea Res. PT II 71–76, 32–48.

Alderkamp, A.-C., van Dijken, G.L., Lowry, K.E., Connelly, T.L., Lagerström, M., Sherrell, R.M., Haskins, C., Rogalsky, E., Schofield, O., Stammerjohn, S.E., 2015. Fe availability drives phytoplankton photosynthesis rates during spring bloom in the Amundsen Sea Polynya, Antarctica. Elem.: Sci. Anthr. 3 (1), 000043.

Anderson, M.J., Willis, T.J., 2003. Canonical analysis of principal coordinates: a useful method of constrained ordination for ecology. Ecology 84 (2), 511–525.

Arrigo, K.R., Brown, Z.W., Mills, M.M., 2014. Sea ice algal biomass and physiology in the Amundsen Sea, Antarctica. Elem.: Sci. Anthr. 2 (1), 000028.

Arrigo, K.R., Lowry, K.E., van Dijken, G.L., 2012. Annual changes in sea ice and phytoplankton in polynyas of the Amundsen Sea, Antarctica. Deep Sea Res. PT II 71, 5–15.

Arrigo, K.R., Mills, M.M., Kropuenske, L.R., van Dijken, G.L., Alderkamp, A.-C., Robinson, D.H., 2010. Photophysiology in two major Southern Ocean phytoplankton taxa: photosynthesis and growth of *Phaeocystis antarctica* and *Fragilariopsis cylindrus* under different irradiance levels. Integr. Comp. Biol. 50, 950–966.

Arrigo, K.R., Robinson, D.H., Worthen, D.L., Dunbar, R.B., DiTullio, G.R., VanWoert, M., Lizotte, M.P., 1999. Phytoplankton community structure and the drawdown of nutrients and CO_2 in the Southern Ocean. Science 283 (5400), 365–367.

Arrigo, K.R., van Dijken, G., Long, M., 2008. Coastal Southern Ocean: a strong anthropogenic CO_2 sink. Geophys. Res. Lett. 35 (21).

Arrigo, K.R., van Dijken, G.L., 2003. Phytoplankton dynamics within 37 Antarctic coastal polynya systems. J. Geophys. Res. -Oceans 108 (C8).

Arrigo, K.R., Worthen, D.L., Robison, D.H., 2003. A coupled ocean-ecosystem model of the Ross Sea: 2. Iron regulation of phytoplankton taxonomic variability and primary production. J. Geophys. Res. -Oceans 108 (No. C7), 3231. http://dx.doi.org/10.1029/2001JC000856.

Arrigo, K.R., Worthen, D., Schnell, A., Lizotte, M.P., 1998. Primary production in Southern Ocean waters. J. Geophys. Res. -Sol. Ea 103 (C8), 15587–15600.

Asper, V.L., Deuser, W., Knauer, G., Lohrenz, S., 1992. Rapid coupling of sinking particle fluxes between surface and deep ocean waters. Nature 357, 670–672.

Boyd, P.W., Jickells, T., Law, C., Blain, S., Boyle, E., Buesseler, K., Coale, K., Cullen, J., De Baar, H., Follows, M., 2007. Mesoscale iron enrichment experiments 1993–2005: synthesis and future directions. Science 315 (5812), 612–617.

Buma, A.G.J., Bano, N., Veldhuis, M.J.W., Kraay, G.W., 1991. Comparison of the pigmentation of two strains of the prymnesiophyte *Phaeocystis* sp. Neth. J. Sea Res. 27, 173–182.

Cavalieri, D.J., Parkinson, C.L., Gloersen, P., Zwally, H.J., 1996, updated yearly. Sea Ice Concentrations from Nimbus-7 SMMR and DMSP SSM/I-SSMIS Passive Microwave Data, Version 1. [2013-2014]. Boulder, Colorado USA. NASA National Snow and Ice Data Center Distributed Active Archive Center. ⟨http://dx.doi.org/10.5067/8GQ8LZQVL0VL⟩ (Date Accessed).

Clarke, K., Ainsworth, M., 1993. A method of linking multivariate community structure to environmental variables. Mar. Ecol. -Prog. Ser. 92, (205-205).

Clarke, K., Gorley, R., 2006. User Manual/Tutorial. PRIMER-E Ltd., Plymouth, 93.

de Baar, H., Buma, A., Nolting, R.F., Cadee, G.C., Jacques, G., Treguer, P.J., 1990. On iron limitation of the Southern Ocean: experimental observations in the Weddell and Scotia Seas. Mar. Ecol. Prog. -Ser. 65, 105–122.

Dortch, Q., Whitledge, T.E., 1992. Does nitrogen or silicon limit phytoplankton

production in the Mississippi River plume and nearby regions? Cont. Shelf Res. 12, 1293–1309.
Ducklow, H.W., Wilson, S.E., Post, A.F., Stammerjohn, S.E., Erickson, M., Lee, S., Lowry, K.E., Sherrell, R.M., Yager, P.L., 2015. Particle flux on the continental shelf in the Amundsen Sea Polynya and Western Antarctic Peninsula. Elem.: Sci. Anthr. 3, 000046.
Eppley, R.W., Holmes, R.W., Strickland, J.D., 1967. Sinking rates of marine phytoplankton measured with a fluorometer. J. Exp. Mar. Biol. Ecol. 1, 191–208.
Fragoso, G.M., Smith, W.O., Jr, 2012. Influence of hydrography on phytoplankton distribution in the Amundsen and Ross Seas, Antarctica. J. Mar. Syst. 89, 19–29.
Garibotti, I.A., Vernet, M., Ferrario, M.E., 2005. Annually recurrent phytoplanktonic assemblages during summer in the seasonal ice zone west of the Antarctic Peninsula (Southern Ocean). Deep-Sea Res. PT I 52, 1823–1841.
Garrison, D.L., Gibson, A., Kunze, H., Gowing, M.M., Vickers, C.L., Mathot, S., Bayre, R.C., 2003. The Ross Sea Polynya Project: diatom- and *Phaeocystis*-dominated phytoplankton assemblages in the Ross Sea, Antarctica, 1994–1996. Biogeochem. Ross. Sea, 53–76.
Gerringa, L.J.A., Alderkamp, A.C., Laan, P., Thuróczy, C.E., De Baar, H.J.W., Mills, M.M., van Dijken, G.L., Haren, H.V., Arrigo, K.R., 2012. Iron from melting glaciers fuels the phytoplankton blooms in Amundsen Sea (Southern Ocean): iron biogeochemistry. Deep-Sea Res. PT II 71–76, 16–31.
Goffart, A., Catalano, G., Hecq, J.H., 2000. Factors controlling the distribution of diatoms and *Phaeocystis* in the Ross Sea. J. Mar. Syst. 27, 161–175.
Ha, H.K., Wåhlin, A.K., Kim, T.W., Lee, S.H., Lee, J.H., Lee, H.J., Hong, C.S., Arneborg, L., Björk, G., Kalén, O., 2014. Circulation and modification of warm deep water on the central amundsen shelf. J. Phys. Oceanogr. 44, 1493–1501.
Hahm, D., Rhee, T.S., Kim, H.C., Park, J., Kim, Y.N., Shin, H.C., Lee, S., 2014. Spatial and temporal variation of net community production and its regulating factors in the Amundsen Sea, Antarctica. J. Geophys. Res. -Oceans 119, 2815–2826.
Hillebrand, H., Dürselen, C.D., Kirschtel, D., Pollingher, U., Zohary, T., 1999. Biovolume calculation for pelagic and benthic microalgae. J. Phycol. 35, 403–424.
Hoppema, M., Anderson, L., 2007. Biogeochemistry of polynyas and their role in sequestration of anthropogenic constituents. Elsevier Oceanogr. Ser. 74, 193–221.
Kang, S.-H., Kang, J.-S., Lee, S., Chung, K.H., Kim, D., Park, M.G., 2001. Antarctic phytoplankton assemblages in the marginal ice zone of the northwestern Weddell Sea. J. Plankton Res. 23, 333–352.
Kim, M., Hwang, J., Kim, H.J., Kim, D., Yang, E.J., Ducklow, H.W., La Hyoung, S., Lee, S.H., Park, J., Lee, S., 2015. Sinking particle flux in the sea ice zone of the Amundsen shelf, Antarctica. Deep-Sea Res. PT I 101, 110–117.
Kropuenske, L.R., Mills, M.M., van Dijken, G.L., Bailey, S., Robinson, D.H., Welschmeyer, N.A., Arrigo, K.R., 2009. Photophysiology in two major Southern Ocean phytoplankton taxa: photoprotection in *Phaeocystis antarctica* and *Fragilariopsis cylindrus*. Limnol. Oceanogr. 54, 1176.
Lancelot, C., Mathot, S., Veth, C., de Baar, H., 1993. Factors controlling phytoplankton ice-edge blooms in the marginal ice-zone of the northwestern Weddell Sea during sea ice retreat 1988: field observations and mathematical modelling. Polar Biol. 13, 377–387.
Lee, Y.C., Park, M.O., Jung, J., Yang, E.J., Lee, S.H., 2015. Taxonomic variability of phytoplankton and relationship with production of CDOM in the polynya of the Amundsen Sea, Antarctica. Deep Sea Res. PT II 123, 30–41.
Mathot, S., Smith, W.O., Carlson, C.A., Garrison, D.L., Gowing, M.M., Vickers, C.L., 2000. Carbon partitioning within *Phaeocystis antarctica* (Prymnesiophyceae) colonies in the Ross Sea, Antarctica. J. Phycol. 36, 1049–1056.
Mendes, C.R.B., Tavano, V.M., Leal, M.C., de Souza, M.S., Brotas, V., Garcia, C.A.E., 2013. Shifts in the dominance between diatoms and cryptophytes during three late summers in the Bransfield Strait (Antarctic Peninsula). Polar Biol. 36, 537–547.
Mills, M.M., Kropuenske, L.R., van Dijken, G.L., Alderkamp, A.-C., Berg, G.M., Robinson, D.H., Welschmeyer, N.A., Arrigo, K.R., 2010. Photophysiology in two Southern Ocean phytoplankton taxa: photosynthesis of *Phaeocystis antarctica* (Prymnesiophyceae) and *Fragilariopsis cylindrus* (Bacillariopyceae) under simulated mixed-layer irradiance. J. Phycol. 46, 114–1127.
Mills, M.M., Alderkamp, A.-C., Thuroczy, C.-E., van Dijken, G.L., Laan, P., de Baar, H.J.W., Arrigo, K.R., 2012. Phytoplankton biomass and pigment responses to Fe amendments in the Pine Island and Amundsen polynyas. Deep-Sea Res. PT II 71–76, 61–76.
Moline, M.A., Claustre, H., Frazer, T.K., Schofield, O., Vernet, M., 2004. Alteration of the food web along the Antarctic Peninsula in response to a regional warming trend. Glob. Change Biol. 10, 1973–1980.
Persons, T., Maita, Y., Lalli, C., 1984. A Manual of Chemical and Biological Methods for Seawater Analysis. Pergamon Press, Oxford, 173.
Pritchard, H., Ligtenberg, S., Fricker, H., Vaughan, D., Van den Broeke, M., Padman, L., 2012. Antarctic ice-sheet loss driven by basal melting of ice shelves. Nature 484 (7395), 502–505.
Raven, J.A., Geider, R.J., 1988. Temperature and algal growth. New Phytol., 441–461.
Rignot, E., Bamber, J.L., Van Den Broeke, M.R., Davis, C., Li, Y., Van De Berg, W.J., Van Meijgaard, E.,, 2008. Recent Antarctic ice mass loss from radar interferometry and regional climate modelling. Nat. Geosci. 1 (2), 106–110.
Rignot, E., Jacobs, S., Mouginot, J., Scheuchl, B., 2013. Ice-shelf melting around Antarctica. Science 341 (6143), 266–270.
Rose, J.M., Feng, Y., Ditullio, G.R., Dunbar, R.B., Hare, C.E., Lee, P.A., Lohan, M., Long, M., Smith, W.O., Jr, Sohst, B., Tozzi, S., Zhang, Y., Hutchins, D.A., 2009. Synergistic effects of iron and temperature on Antarctic phytoplankton and microzooplankton assemblages. Biogeosciences 6 (12), 3131–3147.
Schoemann, V., Becquevort, S., Stefels, J., Rousseau, V., Lancelot, C., 2005. Phaeocystis blooms in the global ocean and their controlling mechanisms: a review. J. Sea Res. 53, 43–66.
Smith, W.O., Jr, Shields, A.R., Peloquin, J.A., Catalano, G., Tozzi, S., Dinniman, M.S., Asper, V.A., 2006. Interannual variations in nutrients, net community production, and biogeochemical cycles in the Ross Sea. Deep-Sea Res. PT II 53 (8–10), 815–833.
Smith, W.O., Dinniman, M.S., Tozzi, S., DiTullio, G.R., Mangoni, O., Modigh, M., Saggiomo, V., 2010. Phytoplankton photosynthetic pigments in the Ross Sea: patterns and relationships among functional groups. J. Mar. Syst. 82 (3), 177–185.
Takahashi, T., Sutherland, S.C., Wanninkhof, R., Sweeney, C., Feely, R.A., Chipman, D.W., Hales, B., Friederich, G., Chavez, F., Sabine, C., 2009. Climatological mean and decadal change in surface ocean pCO_2, and net sea–air CO_2 flux over the global oceans. Deep Sea Res. PT II 56 (8), 554–577.
Taylor, A.G., Landry, M.R., Selph, K.E., Yang, E.J., 2011. Biomass, size structure and depth distributions of the microbial community in the eastern equatorial Pacific. Deep-Sea Res. PT II 58 (3), 342–357.
Tortell, P.D., Long, M.C., Payne, C.D., Alderkamp, A.-C., Dutrieux, P., Arrigo, K.R., 2012. Spatial distribution of pCO_2, ΔO_2/Ar and dimethylsulfide (DMS) in polynya waters and the sea ice zone of the Amundsen Sea, Antarctica. Deep-Sea Res. PT II 71, 77–93.
Tremblay, J.-É., Smith, W., 2007. Primary production and nutrient dynamics in polynyas. Elsevier Oceanogr. Ser. 74, 239–269.
Venables, H., Moore, C.M., 2010. Phytoplankton and light limitation in the Southern Ocean: learning from high-nutrient, high-chlorophyll areas. J. Geophys. Res-Oceans 115 (C2).
Wang, S., Bailey, D., Lindsay, K., Moore, J.K., Holland, M., 2014. Impact of sea ice on the marine iron cycle and phytoplankton productivity. Biogeosciences 11 (17), 4713–4731.
Wright, S.W., van den Enden, R.L., Pearce, I., Davidson, A.T., Scott, F.J., Westwood, K.J., 2010. Phytoplankton community structure and stocks in the Southern Ocean (30–80 °E) determined by CHEMTAX analysis of HPLC pigment signatures. Deep-Sea Res. PT II 57 (9–10), 758–778.
Xu, K., Fu, F.X., Hutchins, D.A., 2014. Comparative responses of two dominant antarctic phytoplankton taxa to interactions between ocean acidification, Warming, Irradiance, And iron availability. Limnol. Oceanogr. 59 (6), 1919–1931.
Yang, E.J., Jiang, Y., Lee, S., 2015. Microzooplankton herbivory and community structure in the Amundsen Sea, Antarctica. Deep-Sea Res. PT II 123, 58–68.